

AST3310 Project 2: Modelling the transport of energy inside a star

(Dated: April 8, 2025)

I. INTRODUCTION

Previously, in the first project of AST3310, we modelled the energy production from the fusion reactions inside the core of a star given its temperature and density. Now, in this second project, I have used a custom python script to model how this energy is transported from the core to the stellar surface through two mechanisms: radiative transport and convective transport.

We keep the same assumptions as in project 1; the atomic species are uniformly distributed in the star such that the mass fractions are independent of position, all the elements are fully ionized, and we disregard the time evolution of the elemental abundances. The mass fractions are taken to be the same as in project 1. Additionally, the stellar plasma is assumed to behave like a monatomic ideal gas and we also assume that there is no heat conduction in the star, only radiation and convection. Finally, we assume that the star is in hydrostatic equilibrium.

Starting from the initial parameters at the surface of the star (given in tab I), the goal was to change M_0 , R_0 , L_0 , T_0 and ρ_0 in order to create a star that satisfies the three criteria:

- the luminosity L , mass m and radius r all go to zero or at least within 5% of their respective initial values;
- the stellar core, considered to be inside the region where $L < 0.995L_0$, reaches out to at least 10% of R_0 ;
- has a continuous convection zone near the surface of the star with a width of at least $0.15R_0$. A small radiation zone at the edge and/or a second convection zone closer to the centre is acceptable, but the convective flux should be small compared to the “main” convection zone near the surface.

Initial parameters	
$M_0^* = M_\odot = 1.989 \times 10^{30}$ kg	
$R_0^* = R_\odot = 6.96 \times 10^8$ m	
$L_0^* = L_\odot = 3.846 \times 10^{26}$ W	
$T_0^* = 5770$ K	
$\rho_0^* = 1.42 \times 10^{-7} \cdot \bar{\rho}_\odot$	

Table I. The initial parameters of the star.

Note: $\bar{\rho}_\odot = 1.408 \times 10^3$ kg m⁻³ is the average density of the Sun.

II. THEORY

A. Calculating the average atomic weight

In the development of this model, we will need to solve for different thermodynamical variables using equations of state, e.g. to find the pressure from the density and temperature. To this end it is practical to define the dimensionless average atomic weight μ as

$$\mu = \frac{\rho/n_{\text{tot}}}{m_u}$$

where ρ is the density, n_{tot} is the total number density of particles and m_u is the atomic mass unit. Since we assume complete ionization of all the elements present in the star, the total number density of particles will be the sum of the number of ions and free electrons $n_{\text{tot}} = n_{\text{ions}} + n_e$. The number density of ions is given by the sum of the number densities of each atomic species

$$n_{\text{ions}} = \sum_i \frac{\phi_i \rho}{m_i} = \sum_i \frac{\phi_i \rho}{A_i m_u}$$

where ϕ_i is the mass fraction of species i , and m_i is the mass of its nucleus. A_i is the number of nucleons.

Each hydrogen atom contributes one electron per nucleus, while each helium 4 and helium 3 atom contributes two, such that $n_{e,1^{\text{H}}} = X\rho/m_u$, $n_{e,4^{\text{He}}} = 2Y\rho/4m_u$ and $n_{e,3^{\text{He}}} = 2Y_{3^{\text{He}}}\rho/3m_u$. For the metals, we can assume that the number of free electrons per ion is approximately half of the number of nucleons such that

$$n_{e,Z_i} \approx \frac{1}{2} A_i \frac{Z_i \rho}{A_i m_u} = \frac{Z_i \rho}{2m_u}$$

where Z_i is the mass fraction of metal i .

Tallying up the total amount of particles, we get

$$\begin{aligned} n_{\text{tot}} &= n_{\text{ions}} + n_e \\ &= (n_{1^{\text{H}}} + n_{e,1^{\text{H}}}) + (n_{2^{\text{He}}} + n_{e,2^{\text{He}}}) \\ &\quad + (n_{3^{\text{He}}} + n_{e,3^{\text{He}}}) + \sum_i (n_{Z_i} + n_{e,Z_i}) \\ &= \frac{2X\rho}{m_u} + \frac{3Y\rho}{4m_u} + \frac{Y_{3^{\text{He}}}\rho}{m_u} + \sum_i \left(\frac{Z_i \rho}{A_i m_u} + \frac{Z_i \rho}{2m_u} \right) \\ &= \frac{\rho}{m_u} \left(2X + \frac{3}{4}Y + Y_{3^{\text{He}}} + \frac{1}{2}Z \right) \end{aligned}$$

In the last step, we have neglected the first terms in the sum over the metals since the mass fractions are tiny compared to the number of nucleons ($A_i \gg Z_i$), and we define the total mass fraction of the metals $Z = \sum_i Z_i$.

From this we see that

$$\mu = \frac{1}{2X + \frac{3}{4}Y + Y_{\text{He}} + \frac{1}{2}Z}$$

In our case, assuming the same mass fractions as in the previous project, we get $\mu = 0.6182$ as the average atomic weight.

B. Integrating the stellar variables

When we assume that there is no heat conduction in the star, the energy produced in the core will be transported out to the surface by two mechanism: electromagnetic radiation and convective transport. In the former, the energy is transported via photon scattering, while in the latter it is transported through the motion of the hot plasma rising and falling in the star. To find where in the star these two mechanisms dominate, we will first have to solve for how the different physical quantities evolve inside the star.

We know that the temperature and pressure will grow exponentially as we approach the center of the star, so we will use the mass m within radius r as our independent variable since it behaves more like the pressure and temperature, according to the lecture notes. In any case, the mass m is still a proxy for r . The change in m as we take an infinitesimal step dm in radius will equal the volume of the spherical shell of width dr times the density $\rho(r)$, i.e. $dm = 4\pi r^2 \rho dr$. Thus, r will evolve with m as described by

$$\frac{\partial r}{\partial m} = \frac{1}{4\pi r^2} \quad (1)$$

The pressure in the star comes from gas pressure P_{gas} and the radiation pressure P_{rad} . By our assumption that the stellar plasma behaves like a monatomic ideal gas, the gas pressure is given by the equation of state $P_{\text{gas}} = \rho k_B T / \mu m_u$ where k_B is Boltzmann's constant. The radiation pressure is given by $P_{\text{rad}} = aT^4/3$ where $a = 4\sigma/c$ with σ being the Stefan-Boltzmann constant and c the speed of light. Hence, the total pressure is given by

$$P = P_{\text{gas}} + P_{\text{rad}} = \frac{\rho k_B T}{\mu m_u} + \frac{4\sigma}{3c} T^4 \quad (2)$$

Since we consider a star in hydrostatic equilibrium, we know that the force resulting from the pressure must equal the gravitational force. The change dP in pressure over the shell of mass dm will therefore have to satisfy

$$\underbrace{4\pi r^2}_{\text{surface area}} dm = -\underbrace{\frac{Gm}{r^2}}_{\text{gravitational force}}$$

and thus we get

$$\frac{\partial P}{\partial m} = -\frac{Gm}{4\pi r^4} \quad (3)$$

The luminosity L of the star represents the energy produced from the fusion reactions per unit time ($L = dE/dt$). This is related to the energy production $\varepsilon = dE/dtdm$ we calculated in the previous project through the relation $dL = \varepsilon dm$. Whence, we get

$$\frac{\partial L}{\partial m} = \varepsilon \quad (4)$$

where ε depends on both the temperature and the density.

C. The temperature of the star

To see how the temperature varies with m , we must consider the two mechanisms for energy transport separately. When there is no convection, the energy is only transported by radiation such that the radiative flux equals the luminosity divided by the surface area: $F_{\text{rad}} = L/4\pi r^2$. The radiative flux can be interpreted as the diffusion of photons from regions of higher photon density (the Sun's core) to regions of lower photon density (the Sun's outer layers): $F_{\text{rad}} = -D|\nabla n|$ where n is the photon density and D is the associated diffusion constant. In the lecture notes it is shown that this leads to the PDE

$$\frac{\partial T}{\partial m} = -\frac{3\kappa L}{256\pi^2\sigma r^4 T^3} \quad (5)$$

However, in the layers where the stellar plasma is unstable under small perturbations, parcels of hot plasma will start to rise upwards towards the outer layers of the star. In fact, when a parcel of plasma experiences a small adiabatic displacement from an initial equilibrium position, its convective stability depends on its density relative to the new surroundings. If the parcel is more dense, it will sink back down. In this case, the initial equilibrium position was stable. If however it is less dense than its new environment, it will continue to rise, indicating an unstable equilibrium. As the parcel rises through the star it will cool due to adiabatic expansion (the pressure decreases towards the outer layers) and radiation.

If we define the temperature gradient

$$\nabla \equiv \left(\frac{\partial \ln T}{\partial \ln P} \right)_s$$

the instability criterion can be formulated as $\nabla^* > \nabla_{\text{ad}}$, with the $*$ in superscript referring to the actual temperature gradient of the star, and "ad" in subscript refers to the adiabatic temperature gradient (no cooling due to radiation).

The latter is given in the lecture notes to be

$$\nabla_{\text{ad}} = \frac{P\delta}{T\rho c_P}$$

For a monatomic ideal gas, the specific heat at constant pressure is $c_P = 5k_B/2\mu m_u$ and

$$\begin{aligned}\delta &\equiv -\left(\frac{\partial \ln \rho}{\partial \ln T}\right)_P = -\frac{T}{\rho} \left(\frac{\partial \rho}{\partial T}\right)_P \\ &= -\frac{T}{\rho} \left(-\frac{P\mu m_u}{k_B T^2}\right) \\ &= \frac{T}{\rho} \cdot \frac{\rho}{T} = 1\end{aligned}$$

If the instability criterion is not satisfied, we use the eq. (5) for the temperature. The resulting temperature gradient is

$$\begin{aligned}\nabla_{\text{stable}} &= \left(\frac{\partial \ln T}{\partial \ln P}\right)_s \\ &= \frac{P \partial T}{T \partial P} = \frac{P \partial T}{T \partial m} \frac{1}{(\partial P / \partial m)} \\ &= \frac{P}{T} \cdot \left(-\frac{3\kappa L}{256\pi^2\sigma r^4 T^3}\right) \cdot \left(-\frac{4\pi r^4}{Gm}\right) \\ &= \frac{3\kappa LP}{64\pi Gm\sigma T^4}\end{aligned}\quad (6)$$

On the other hand, if the instability criterion *is* satisfied, we must use the expression for $\partial T / \partial m$ resulting from ∇^* :

$$\begin{aligned}\nabla^* &= \left(\frac{\partial \ln T}{\partial \ln P}\right)_s \\ &= \frac{P \partial T}{T \partial m} \frac{1}{(\partial P / \partial m)} \\ \Rightarrow \frac{\partial T}{\partial m} &= \nabla^* \frac{T \partial P}{P \partial m}\end{aligned}\quad (7)$$

To get the value of ∇^* , we first have to introduce another temperature gradient; the gradient ∇_p which describes the temperature of the parcel of plasma as it rises. If we then define $\xi \equiv (\nabla^* - \nabla_p)^{1/2}$, we can solve for ξ in the equation

$$\xi^3 + \frac{U}{l_m^2} \xi^2 + 4 \left(\frac{U}{l_m^2} \right)^2 \xi - \frac{U}{l_m^2} (\nabla_{\text{stable}} - \nabla_{\text{ad}}) = 0 \quad (8)$$

and then find ∇^* using the solution for ξ as

$$\nabla^* = \xi^2 + 4 \frac{U}{l_m^2} \xi + \nabla_{\text{ad}} \quad (9)$$

The derivations and explanations of eqs. (8) and (9) are given in the appendix A.

III. METHOD

A. Implementing dynamic step size

To numerically integrate the stellar variables over m , I decided for simplicity to use the Forward Euler method

for each of the equations: $\partial r / \partial m$ (eq. 1), $\partial P / \partial m$ (eq. 3), $\partial L / \partial m$ (eq. 4), and $\partial T / \partial m$ (either eq. 5 or eq. 7 depending on whether the layer is convectively stable or not). The change in variable V_i is given by

$$dV_i = \frac{\partial V_i}{\partial m} dm$$

in the Forward Euler method.

For the this method to be sufficiently accurate when dealing with physical quantities that can change by several orders of magnitude over small changes in m (especially towards the center of the star), we must implement a dynamic step size for each step in mass dm as described in the project description to prevent the variables from “blowing up” towards the center. At each step in the integration, the model calculates

$$dm_i = p \left| \frac{V_i}{\partial V_i / \partial m} \right|$$

for each variable V_i and chooses the minimal dm_i to assure that all the variables are well behaved. The parameter p is a measure of the size of the dynamic step length; I ended up using $p = 0.003$ for the solutions to converge.

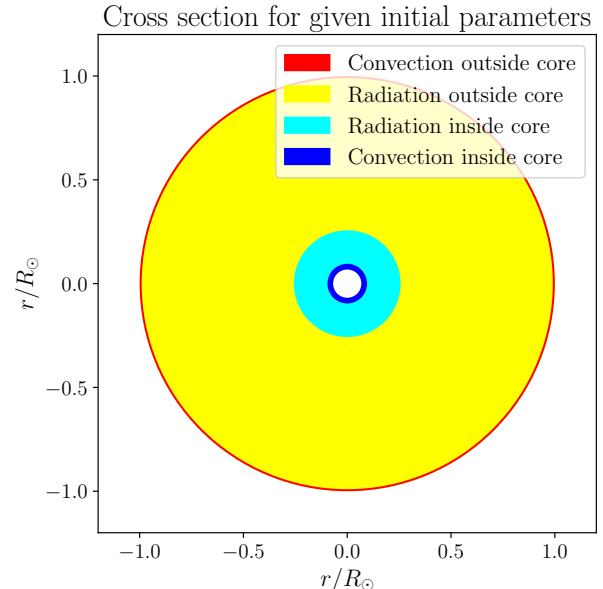


Figure 1. The cross section of the star with initial conditions given in tab. I.

B. Checking the validity of the model

Before adjusting the initial conditions of the star to reach the goals of the project, I implemented the sanity checks described in the project description to check the

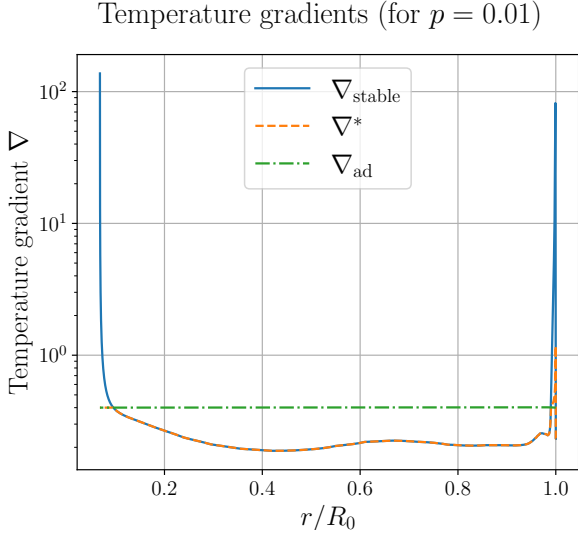


Figure 2. Temperature gradients of the star with initial conditions described in tab. I.

validity of the solutions produced by the numerical integrations. The model passed all the checks with no values differing more than 5% from the reference values.

When I plotted the cross section of the star with the initial condition given in tab. I, the resulting figure (fig. 1) matches the cross section shown in the project description. Also, the plot of the resulting temperature gradients for the star (fig. 2) reproduces almost exactly the figure shown in the project description. These tests gave me confidence to start searching for the optimal initial parameters.

C. Finding the optimal star

The first step in trying to find the initial conditions of the optimal star that satisfies the goals presented in the introduction was to investigate the isolated effect of changing each of the parameters one by one and keeping the others unchanged. To do this, I defined the scaling factors $\chi_i = V_{i,0}/V_{i,0}^*$ for each initial value $V_{i,0}$ (the values of $V_{i,0}^*$ are the ones given in tab. I). I then found the solutions when setting $V_{i,0} = \chi_{\text{par}} V_{i,0}^*$ with $\chi_{\text{par}} = 0.1, 1, 10$ and plotted the “star zone” parameter as a function of r/R_0 . The star zones are numbered 0 through 3 and are defined as:

- Star zone 0: inside the core ($L < 0.995L_0$) and convection ($F_{\text{con}} > 0$).
- Star zone 1: inside the core ($L < 0.995L_0$) and radiation ($F_{\text{con}} = 0$).
- Star zone 2: outside the core ($L \geq 0.995L_0$) and radiation ($F_{\text{con}} = 0$).
- Star zone 3: outside the core ($L \geq 0.995L_0$) and convection ($F_{\text{con}} > 0$).

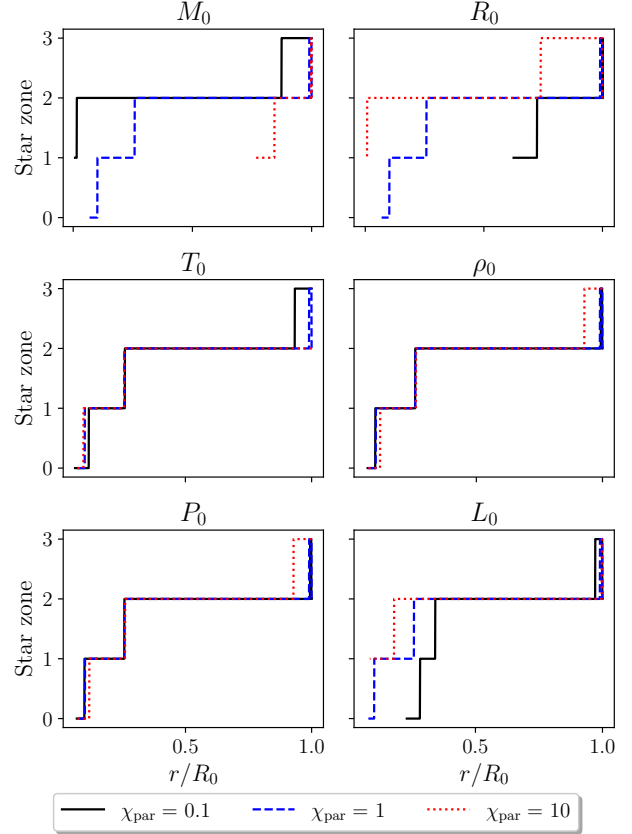


Figure 3. Star zone plotted as a function of r/R_0 when scaling the initial parameters by $\chi_{\text{par}} = 0.1, 1, 10$ one by one. Each of the frames show the spatial extent of the star zones when *only* changing the initial value of the variable corresponding to that frame.

The expression for the convective flux F_{con} , as well as for the radiative flux F_{rad} , is given in the appendix A. The resulting plot is shown in fig. 3.

Note that in some of the cases, the integration never made it past the thresholds of L , r and m reaching $\leq 5\%$ of their initial values. In these cases, when this condition was saturated after before reaching the thresholds, I had to stop the numerical integration over m by checking when the step size was negligible compared to the total mass of the star. I arbitrarily chose to break the integration when $dm < 10^6$ kg if the condition wasn't satisfied yet. This was a practical fix to the problem and I figured that the most important thing was to observe the qualitative effect for the outer convective layer anyways.

When we observe the graphs in fig. 3, we notice that changing the mass M_0 or radius R_0 by even one order of magnitude can make the model unstable, stopping the integration early and not reaching the desired threshold for L , r and m . Increasing R_0 however still widens the outer convective region of the star. This is because the outer layers of a big star will be much cooler and have lower density and pressure. The radiative flux will there-

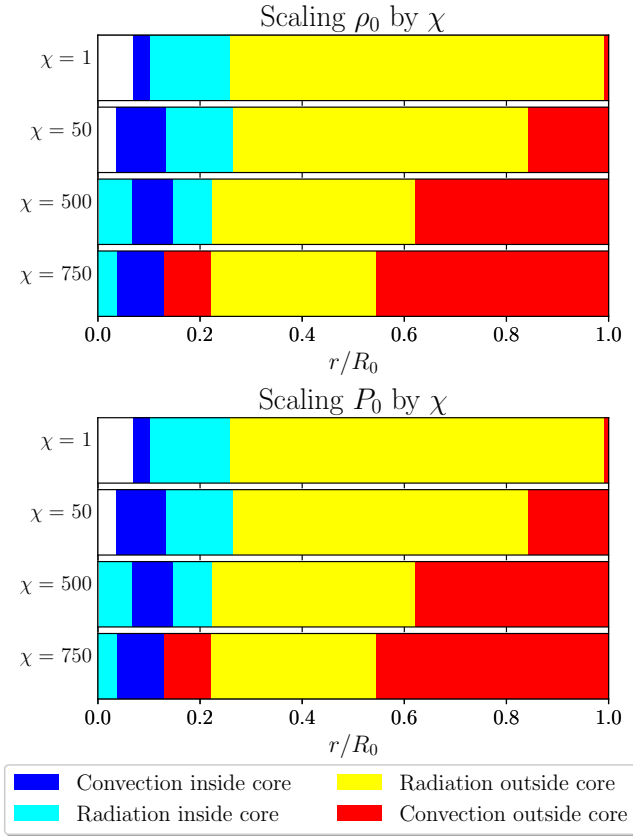


Figure 4. The layering of the resulting stars when scaling ρ_0 and P_0 by $\chi = 1, 50, 500, 750$. Note: plotting both may be redundant when, but it emphasizes the linear relation between the two initial values.

fore be considerably lower compared to the convective flux. The weaker gravity will also make it easier for the buoyant force acting on the parcels of plasma to make it rise.

Scaling the temperature T_0 seems to have a minimal effect on spatial extent of the star zones. However, decreasing the luminosity L_0 greatly increases the extent of the core. This is because the change in L due to the energy production ε will be greater relative to the magnitude of L such that it pass the limit $L < 0.995L_0$ faster once ε starts to increase towards the center.

Lastly, we notice that scaling the density ρ_0 and P_0 yields very similar outcomes. This is because of the linear relationship (for constant T_0) between the two variables in the equation of state (2). We see that increasing either of them increases the width of the outer convective layer quite effectively. To further investigate the effect of bigger scaling factors for ρ_0 and P_0 , I plotted the 1D version of the cross section for $\chi = 1, 50, 500, 750$ in fig. 4. We notice that big scaling factors substantially increases the width of the outer convective layer, while maintaining a sizeable core (reaching out to $\sim 0.2R_0$). The effect on the outer convective layer can be under-

stood through the expression for ∇_{stable} (eq. 6). Scaling either ρ_0 or P_0 directly will increase the initial ∇_{stable} gradient. This means that it will take longer for it to pass below the value of ∇_{ad} , and thus we will have a wider convectively unstable region ($\nabla_{\text{stable}} > \nabla_{\text{ad}}$).

After these discoveries I decided it was best to find the parameters of the optimal star by trial and error. The most effective way to increase the width of the outer convective layer was scaling the density ρ_0 and R_0 . I also ended up playing around with the values of L_0 to adjust the size of the core and ensure that L, r and m passed below 5% of their initial values. The trial and error was done in line with the rules imposed by the project description: $0.2 \leq \chi_{R_0}, \chi_{L_0} \leq 5$ and I could change ρ_0 as much as I wanted.

IV. RESULTS

A. The optimal star

All three criteria put forth in the introduction were satisfied when setting $\chi_{R_0} = 1.3$, $\chi_{\rho_0} = 25$ and $\chi_{L_0} = 1.2$, or in terms of R_\odot , $\bar{\rho}_\odot$ and L_\odot :

$$R_0 = 1.3R_\odot, \quad \rho_0 = 3.55 \times 10^{-6} \cdot \bar{\rho}_\odot, \quad L_0 = 1.2L_\odot$$

The rest of the initial values were taken from tab. I. This is what I will refer to as the optimal star.

Looking at the cross section and the 1D star zone plot shown in fig. 5, we see that the optimal star has a continuous convection zone near the surface of the star with a width of $0.152R_0$ and a stellar core reaching out to $0.194R_0$, so the last two goals were met. Fig. 6 shows the stellar variables plotted over r/R_0 . These show the L, m and r going to zero towards the center. The final values of these three were

$$\frac{L}{L_0} = 0.050, \quad \frac{m}{M_0} = 0.030, \quad \frac{r}{R_0} = 0.002$$

Thus the first goal was also reached.

B. Temperature gradients, relative energy production, and fluxes of the optimal star

From the solutions for the stellar variables of the optimal star, I calculated the temperature gradients ∇_{stable} , ∇^* and ∇_{ad} and plotted them as a function of r/R_0 in fig. 7. In fig. 8 I calculated the radiative and convective energy fluxes and plotted their relative sizes (normalized to $F_{\text{tot}} = F_{\text{rad}} + F_{\text{con}} = L/4\pi r^2$). Lastly, I used the model developed in the previous project to plot the relative energy production of the PP chains and the CNO cycle as a function of r/R_0 in fig. 9.

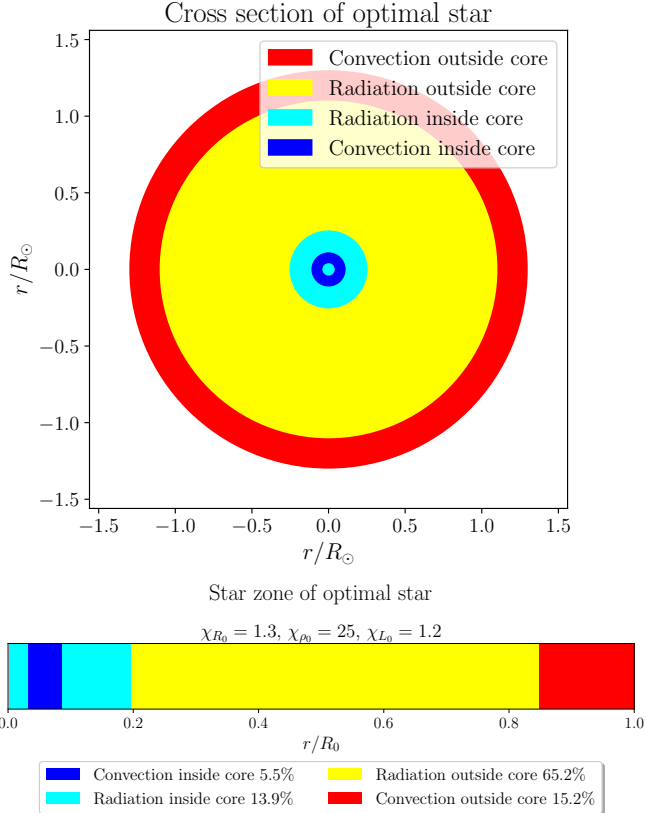


Figure 5. Top: the cross section of the optimal star. Bottom: the 1D plot of the star zones in the optimal star along with the percentages of their width compared to the total radius R_0 .

V. DISCUSSION

A. Calculating the energy production ε

During the development of the model I had some complications with using the energy production ε calculated by the model from the previous project. Thus, due to time constraints, I quickly abandoned the method and decided to interpolate the ε -values given in the txt-file accompanying the project description instead. This worked tremendously well.

B. The physical validity of the model and the optimal star

To check the physical validity of the solution we get for the optimal star, we can inspect the plot of the main parameters (fig. 6). We immediately notice that the mass m and the luminosity L go to zero as we approach the center of the star. The luminosity drops rapidly after passing $< 0.2R_0$. This makes sense since this is around the boundary of the core (see fig. 5), where almost all the

fusion reactions (i.e. energy production) happen. The temperature T , the density ρ and the pressure P also behave as we should expect; they all increase exponentially towards the center of the star.

Our star's central temperature reaches $T_{\text{center}} = 5.17 \times 10^7$ K which is a little over three times that of the Sun with its central temperature being around $T_{\odot,\text{center}} = 1.57 \times 10^7$ K [1]. The temperature difference can be explained by the difference in density near the center. For our star, the density reaches $\rho_{\text{center}} = 4.79 \times 10^6 \text{ kg/m}^3$, while for the Sun it is around $\rho_{\odot,\text{center}} \sim 1.5 \times 10^5 \text{ kg/m}^3$ [1]. Since we are assuming an ideal gas, the higher density results in a higher temperature. Nevertheless, the final values of the temperature and the density are comparable in terms of order of magnitude. This bodes well for the physical validity of our model.

We can also compare the cross section of our star (fig. 5) to that of the Sun. The Sun has a core reaching out to about $0.24R_\odot$ [1], which is comparable to our star's core that reaches out to $0.194R_0$. Since our star is slightly bigger and has a higher luminosity, it makes sense that the relative size of the core is a bit smaller than for the Sun.

The radiative zone outside of the core has a width of about $0.45R_\odot$ in the Sun [1], while the one in our star has a width of $0.652R_0$. This discrepancy can probably be explained by the higher density and pressure in the outer regions of our star compared to the Sun (the initial density ρ_0 is 25 times larger for our star). Another reason might be that our assumption of location-independent mass fractions of the atomic species in the star. In reality, the metals should be more concentrated towards the center of the star and this will alter the value of the average atomic weight μ .

Lastly the outer convective zone of the Sun stretches from about $0.7R_\odot$ to near the surface [1], i.e. roughly 30% of the radius. Our star's convective zone is quite a lot smaller at 15.2% of the radius.

C. The temperature gradients and the relative fluxes

The star is convectively unstable where the instability criterion $\nabla^* > \nabla_{\text{ad}}$ which in practice is where $\nabla_{\text{stable}} > \nabla_{\text{ad}}$, since $\nabla_{\text{stable}} \geq \nabla^*$. We thus see a clear connection between the temperature gradient plot (fig. 7) and the star zones (fig. 5). The spatial extent of the two convective zones in our star mirrors where the graph of ∇_{stable} lies above ∇_{ad} .

The relative energy fluxes (fig. 8) also reveal the same spatial extents of the star zones as the cross section and the temperature gradients; the convective flux F_{con} is only non-zero in the convective regions of the star, which lines up perfectly with the boundaries shown in the two other figures (fig. 5 & 7). The relative energy flux plot

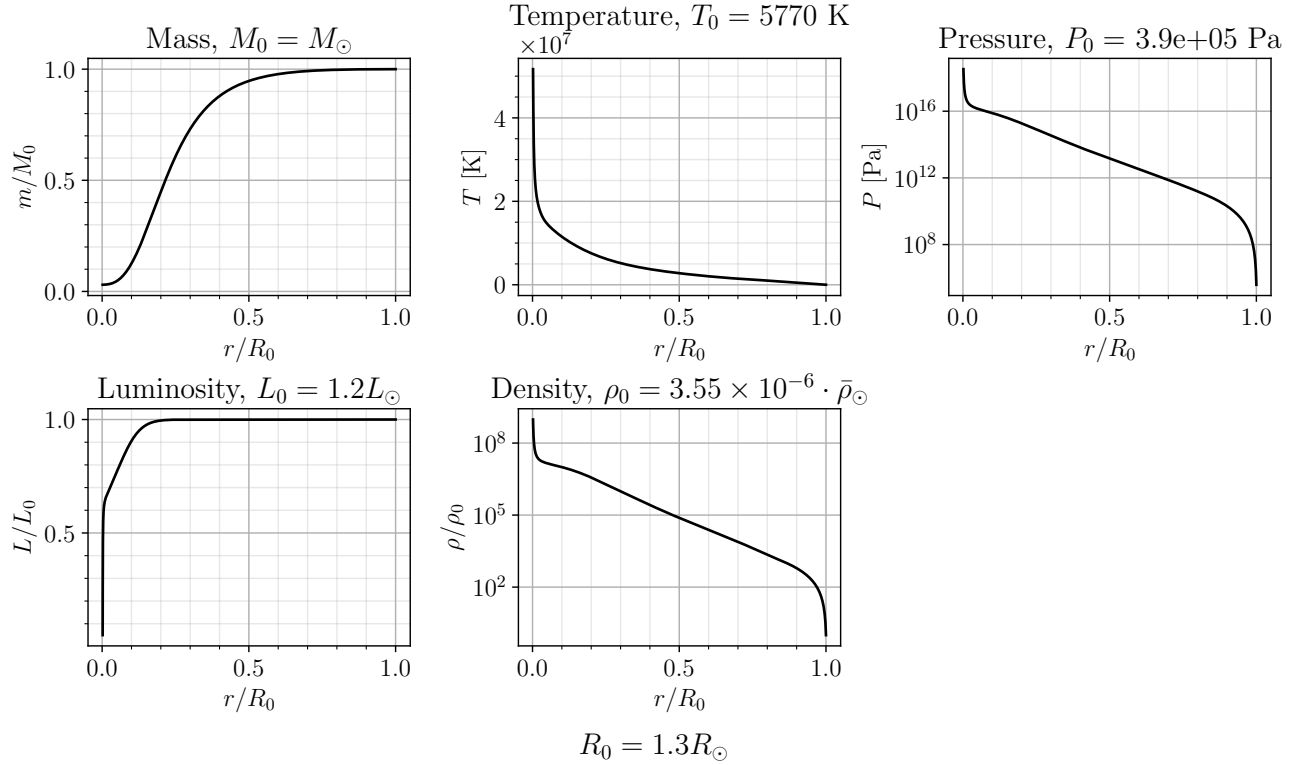


Figure 6. The stellar variables of the optimal star plotted over r/R_0 .

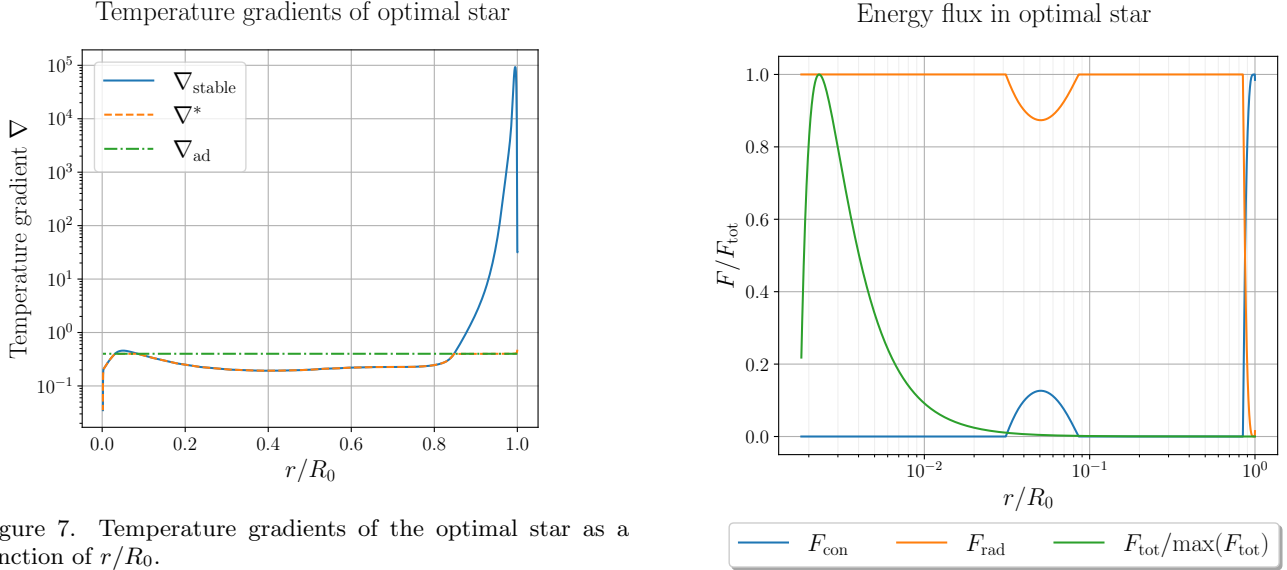


Figure 7. Temperature gradients of the optimal star as a function of r/R_0 .

also reveals that the convective flux is only dominant in the outer-most convective layer ($r \gtrsim 0.9R_0$), so even though we also have a convective zone inside the core, the radiative flux still dominates here and is responsible for over 90% of the total energy flux in this region.

Figure 8. Relative energy fluxes for the optimal star as a function of r/R_0 . I have also included the total flux F_{tot} normalized to its maximum.

D. The relative energy production

In fig. 9, we see that the total energy production normalized to its maximum is negligible above 0.3% of R_0 .

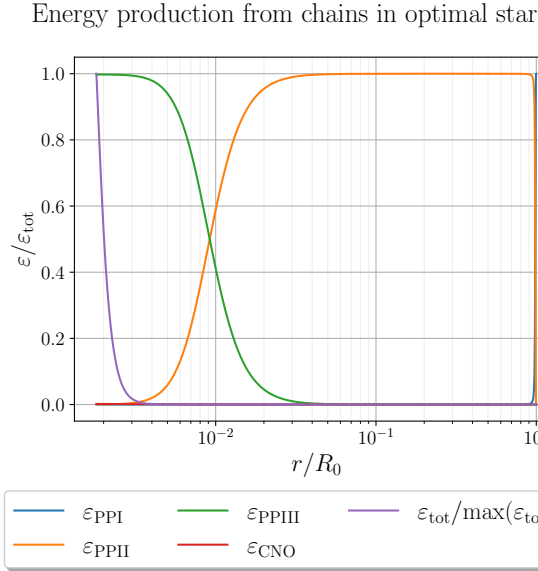


Figure 9. Relative energy production of the PP chains and the CNO cycle as a function of r/R_0 .

In this inner-most region of the star, the energy production is almost entirely dominated by the PPIII chain. The temperature inside this region is around $T \sim 5 \times 10^7$ K, while the density is around $\rho \sim 4.5 \times 10^6 \text{ kg/m}^3$. Plotting the relative energy production as a function of T for $\rho = 4.5 \times 10^6 \text{ kg/m}^3$ (fig. 10), we see that the model developed in the previous project predicts that PPIII should indeed dominate under these conditions.

Further out in the star, the PPII chain dominates and all the way out towards the edge, the PPI chain dominates. This makes physical sense and is in agreement with the tendency shown in fig. 10 as the temperature and density drops rapidly outwards.

VI. CONCLUSION

In this project, we successfully modeled stellar energy transport mechanisms, achieving the goals of a continuous outer convection zone (width $\geq 0.15R_0$), a core extending to $\geq 10\%$ of R_0 , and convergence of L , m , and r to within 5% of their initial values. The optimal star, with initial parameters $R_0 = 1.3R_\odot$, $\rho_0 = 3.55 \times 10^{-6} \bar{\rho}_\odot$, and $L_0 = 1.2L_\odot$, demonstrated physically plausible behavior, including dominant PPIII chain energy production in the inner parts of the core and radiative/convec-

tive flux distributions consistent with theoretical expectations. The results align with stellar physics principles, validating the model's robustness. Further refinements could address assumptions like uniform mass fractions to enhance accuracy.

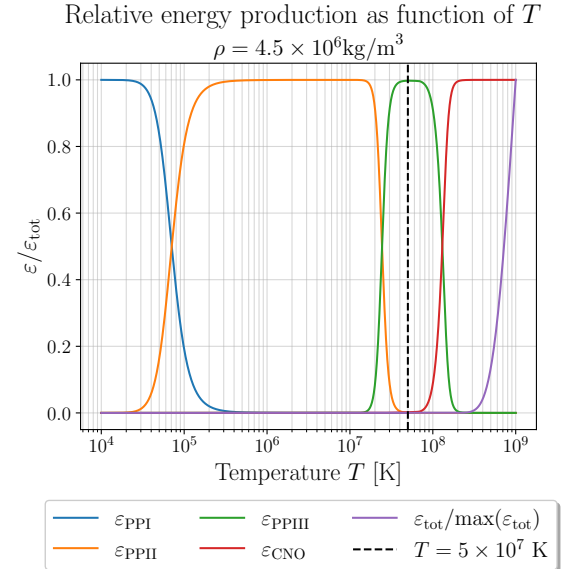


Figure 10. Relative energy production as a function of temperature T for $\rho = 4.5 \times 10^6 \text{ kg/m}^3$. The plot was produced using the model developed in the previous project.

VII. REFLECTION

All things considered, I am very pleased with the results in this project. As was also the case in the first project, most of my time was spent debugging the code and trying to structure it neatly. This time I found it harder to structure the code and make it short and readable.

I also spent quite a long time being confused as to why we check for convective instability using the condition $\nabla_{\text{stable}} > \nabla_{\text{ad}}$ instead of $\nabla^* > \nabla_{\text{ad}}$. I know that $\nabla_{\text{stable}} > \nabla^*$, such that $\nabla_{\text{stable}} \leq \nabla_{\text{ad}} \implies \nabla^* \leq \nabla_{\text{ad}}$, but it is still unclear to me why ∇^* cannot be less than ∇_{ad} without $\nabla_{\text{stable}} \leq \nabla_{\text{ad}}$.

In the derivations of the solutions to exercises 5.11-5.13 written in the appendix, it was also a bit tricky to know how much detail was necessary. I have tried to present the solutions without having to summarize the whole chapter in the lecture notes.

[1] Sun. Wikipedia, Apr 2025. <https://en.wikipedia.org/wiki/Sun>.

Appendix A: Derivation of 3rd order polynomial equation for the temperature gradient of the star

Eq (5.86) in the lecture notes states that the total energy flux in the convection zone of the star is related to the temperature gradient ∇_{stable} needed for all the energy to be carried by radiation through the expression

$$F_{\text{rad}} + F_{\text{con}} = \frac{16\sigma T^4}{3\kappa\rho H_P} \nabla_{\text{stable}}$$

where F_{rad} and F_{con} are the fluxes of the energy carried by radiation and convection respectively. These are given in eq (5.87) and (5.85):

$$\begin{aligned} F_{\text{rad}} &= \frac{16\sigma T^4}{3\kappa\rho H_P} \nabla^* \\ F_{\text{con}} &= \rho c_P T \sqrt{g\delta} H_P^{-3/2} \left(\frac{l_m}{2} \right)^2 (\nabla^* - \nabla_p)^{3/2} \end{aligned}$$

Combining these three equations, we get

$$\begin{aligned} \frac{16\sigma T^4}{3\kappa\rho H_P} \nabla^* + \rho c_P T \sqrt{g\delta} H_P^{-3/2} \left(\frac{l_m}{2} \right)^2 (\nabla^* - \nabla_p)^{3/2} &= \frac{16\sigma T^4}{3\kappa\rho H_P} \nabla_{\text{stable}} \\ \Leftrightarrow (\nabla^* - \nabla_p)^{3/2} &= \frac{1}{\rho c_P T \sqrt{g\delta} H_P^{-3/2}} \cdot \frac{16\sigma T^4}{3\kappa\rho H_P} \left(\frac{2}{l_m} \right)^2 (\nabla_{\text{stable}} - \nabla^*) \\ &= \frac{64\sigma T^3}{3\kappa\rho^2 c_P} \left(\frac{H_P}{g\delta} \right)^{1/2} l_m^{-2} (\nabla_{\text{stable}} - \nabla^*) \end{aligned} \quad (\text{A1})$$

Next, the difference between the temperature gradient ∇_p of the parcel of plasma and that of the adiabatic ∇_{ad} can be written as

$$(\nabla_p - \nabla_{\text{ad}}) = (\nabla^* - \nabla_{\text{ad}}) - (\nabla^* - \nabla_p)$$

If we then introduce the solution $\xi \equiv (\nabla^* - \nabla_p)^{1/2}$ and use the expression for the $(\nabla_p - \nabla_{\text{ad}})$ term given in eq (5.84) in the lecture notes, we get

$$\underbrace{\frac{64\sigma T^3}{3\kappa\rho^2 c_P} \left(\frac{H_P}{g\delta} \right)^{1/2} \left(\frac{S}{Ql_m d} \right)}_{\equiv U} \xi = (\nabla^* - \nabla_{\text{ad}}) - \xi^2$$

$$\Leftrightarrow \xi^2 + \frac{U}{l_m^2} \frac{Sl_m}{Qd} \xi - (\nabla^* - \nabla_{\text{ad}}) = 0 \quad (\text{A2})$$

Continuing, using the definition of ξ and U , we can further simplify eq (A1) as

$$\xi^3 - \frac{U}{l_m^2} (\nabla_{\text{stable}} - \nabla^*) = 0$$

If we then add this equation to eq (A2) multiplied by U/l_m^2 , we get

$$\xi^3 + \frac{U}{l_m^2} \xi^2 + \frac{Sl_m}{Qd} \left(\frac{U}{l_m^2} \right)^2 \xi - \frac{U}{l_m^2} (\nabla_{\text{stable}} - \nabla_{\text{ad}}) = 0$$

We assume that the parcel of plasma is perfectly spherical with radius $r_p = l_m/2 = d/2$. The surface of the parcel is then $S = 4\pi r_p^2$ and Q is just the cross sectional area, i.e. $Q = \pi r_p^2$. With this assumption, the factor Sl_m/Qd in front of the order one term reduces to

$$\frac{Sl_m}{Qd} = \frac{4\pi r_p^2 \cdot 2r_p}{\pi r_p^2 \cdot 2r_p} = 4$$

Thus we end up with a polynomial equation of order three for $\xi \equiv (\nabla^* - \nabla_p)^{1/2}$

$$\xi^3 + \frac{U}{l_m^2} \xi^2 + 4 \left(\frac{U}{l_m^2} \right)^2 \xi - \frac{U}{l_m^2} (\nabla_{\text{stable}} - \nabla_{\text{ad}}) = 0$$

Note that we can get rid of the of the pressure scale length H_P and the mixing length l_m in the expression for U/l_m^2 using their definitions:

$$\begin{aligned} H_P &\equiv -P \frac{\partial r}{\partial P} = -P \frac{\partial r}{\partial m} \frac{\partial m}{\partial P} \\ &= -P \frac{1}{4\pi r^2 \rho} \cdot \left(-\frac{4\pi r^4}{Gm} \right) \\ &= \frac{Pr^2}{Gm\rho} = \frac{P}{g\rho} \end{aligned}$$

and

$$l_m = \alpha_{l_m} H_P \stackrel{\alpha_{l_m}=1}{=} \frac{P}{g\rho}$$

such that

$$\frac{U}{l_m^2} = \frac{64\sigma T^3}{3\kappa\rho^2 c_P} \left(\frac{H_P}{g\delta} \right)^{1/2} l_m^{-2} = \frac{64\sigma T^3 g}{3\kappa c_P P^2} \left(\frac{P}{\rho\delta} \right)^{1/2}$$

This is the way I calculated the coefficient in the code.

Although this equation has three solutions per the fundamental theorem of algebra, we can quite easily show that it only has *one* real solution, which is the only one

we care about¹. If we look for the extremum points of the polynomial by setting the derivative to zero, we get

$$3\xi^2 + 2\frac{U}{l_m^2}\xi + 4\left(\frac{U}{l_m^2}\right)^2 = 0$$

This has no real solutions, since the discriminant is negative

$$\Delta = b^2 - 4ac = 4\left(\frac{U}{l_m^2}\right)^2 - 48\left(\frac{U}{l_m^2}\right)^2 < 0$$

Thus, the polynomial has no extremum points and must therefore either be strictly increasing or decreasing and hence cannot cross zero more than exactly once.

Once we have found the real solution for ξ , we can calculate ∇^* from

$$\nabla^* = \xi^2 + \nabla_p = \xi^2 + (\nabla_p - \nabla_{ad}) + \nabla_{ad}$$

Inserting the expression for $(\nabla_p - \nabla_{ad})$ using the U/l_m^2 coefficient and $Sl_m/Qd = 4$, we get

$$\nabla^* = \xi^2 + 4\frac{U}{l_m^2}\xi + \nabla_{ad}$$

□

¹ I felt it was more relevant to argue why it only has one viable solution at the end, because this argument better explains how I actually find the solution to the equation in the code.